Electronic Supplementary Material (ESI) for Environmental Science: Processes & Impacts.

Supporting Information

for

Impact of Dissolved O_2 on Phenol Oxidation by δ-MnO_2

*Erdan Hu, Shangyue Pan, Wenzhong Zhang, Xinglei Zhao, Bang Liao, Feng He**

College of Environment, Zhejiang University of Technology, Hangzhou 310014, China

Date: 10/22/2019

Number of Pages: 16

Number of Tables: 2

Number of Figures: 10

Chemicals. Phenol (99%), hydroquinone (99%), p-benzoquinone (99%) and 4,4'-biphenol (99%) were purchased from J&K Scientific Ltd. (Beijing, China); HPLC grade methanol and dichloromethane were supplied by CNW Technologies (Dusseldorf, Germany); Manganese chloride (99%), sodium hydroxide (98%) and ammonium acetate (99%) were obtained from Aladdin Bio-Chem. Technology Co., Ltd. (Shanghai, China); Potassium permanganate (99.5%) was purchased from Xiaoshan Chemical Reagent Co., Ltd. (Zhejiang, China); Acetic acid (99.5%) was supplied by Lingfeng Chemical Reagent Co., Ltd. (Shanghai, China); Boric acid (99.5%) was obtained from Macklin Bio-Chem. Co., Ltd. (Shanghai, China); Sodium nitrate (99%) was purchased from Guanghua Sci-Tech Co., Ltd. (Guangdong, China). Pure (> 99%) manganese oxides (MnO, Mn_2O_3, and MnO_2) were purchased from Macklin Bio-Chem. Co., Ltd. (Shanghai, China) to be used as XPS references. All chemicals were used as received. Laboratory distilled, deionized water (resistivity of 18.2 MΩ·cm) was used in preparation of all aqueous solutions.

Buffer Selection. Preliminary experiments were conducted to assess whether the presence of buffers affected the degradation of phenol by δ-MnO_2. Results in **Figure S1** indicated that acetate (pH 5.5) had negligible effect on the oxidation of phenol. While it appears that ammonium acetate (pH 7.0) and borate (pH 8.5) buffers enhanced the oxidation rates of phenol, which was attributed to the maintenance of pH by the buffers. As pH could increase by about 1~3 units without buffers, resulting in a decrease of phenol degradation kinetic during the reaction. The other three commonly used buffers, 2-(N-morpholino)ethanesulfonic acid (MES, pH 5.5), 4-(2-hydroxyethyl)-1-piperazineethanesulfonic acid (HEPES, pH 7.0), and N-(2-hydroxyethyl)piperazine-N′-(3-propanesulfonic acid) (HEPPS, pH 8.5) strongly

inhibited phenol oxidation, which could be due to their competition for reactive sites and reduction of δ-MnO_2 [1,2]. Thus we used acetate, ammonium acetate, and borate buffers to maintain pH in the subsequent experiments.

Identification of Phenol Degradation Products. The identification and quantification of phenol degradation products were accomplished through gas chromatography/mass spectrometry (GC/MS) after extraction with dichloromethane. Phenol and its degradation products were analyzed on an Agilent 7890B-5977B GC/MS with a HP-5 capillary column (30 m × 0.25 mm i.d., 0.25 μm film thickness; J&W Scientific, Folsom, CA, USA). 1μL of the samples was injected splitless at injector temperature of 280 °C. The GC was programmed from 50 °C to 270 °C (8 °C/min). The mass spectrometer was operated with electron impact (EI) ionization at 70 eV, with a solvent delay of 4 min. The full scan mode (50–550 amu, 1.5 scans/s) was used for screening and library-assisted identification of phenol degradation products. Selected ion monitoring (SIM) mode was used for quantitative analysis using m/z 94.0 for phenol (C_2H_6O), m/z 108.0 for its degradation product benzoquinone ($C_6H_4O_2$), m/z 110.0 for hydroquinone ($C_6H_6O_2$), and m/z 186.1 for 4,4'-biphenol ($C_{12}H_{10}O_2$). Blanks and standards were also run regularly.

Iodine Titration. Iodine titration was performed to determine the Mn average oxidation state (Mn AOS) of the control and reacted samples as described by Villalobos et al., [3]. Briefly, 100 mg of Mn oxides was suspended in 50 mL water in a 100 mL volumetric flask, followed by the addition of 10 mL of 4 M NaI, and 5 mL of 2 M H_2SO_4. The water were purged with N_2 for more than 3 hours before used to prepare solutions. After the sample was completely dissolved, the solution was titrated with a 0.18 M $Na_2S_2O_3$ solution. The experiments were

repeated three times. Mn AOS were calculated as follows:

$$\text{Mn AOS} = 4*(1-\alpha) + 3*\alpha$$

where α is the mole fraction of Mn(III) and is equal to:

$$\alpha = 2 - \text{mol } Na_2S_2O_3 / \text{mol Mn}$$

FTIR Analysis. The change of δ-MnO_2 after reduction by phenol was further characterized by FTIR spectrum (**Figure S8**). In the 750-400 cm^{-1} region, which are assigned to Mn-O stretching vibrations, two peaks were observed at 517 and 461 cm^{-1}. The strong broad peak at 3393 cm^{-1} corresponded with the stretching vibration of the adsorbed water and interlayer water molecules. The peak at 1627 cm^{-1} was due to the bending vibration of water molecules [4-6]. It can be seen that after reaction with phenol, the peak at 461 cm^{-1} significantly weakened relative to the original δ-MnO_2, especially under anoxic conditions, indicating that Mn–O groups on the δ-MnO_2 surface might be active sites for phenol sorption and oxidation. It was reported that differences of the Mn-O bonding environments within manganese oxide could be caused by structural disorder, changes in the Mn(III)/Mn(IV) ratio or the replacement of Mn cations with vacancies in the octahedral sheets during the reaction processes [6]. Under oxic conditions, phenol was oxidized slower than under anoxic condition, thus consumed less reactive sites. As a result, the weakening of the signal at peak 461 cm^{-1} was not as significant as that under anoxic conditions. At pH 8.5, although less reactive sites were consumed by phenol oxidation, the peak intensity at 461 cm^{-1} decreased more seriously compared to pH 5.5 and 7.0 under both oxic and anxic conditions, which may be due to the more severe oxidation and precipitation of reduced Mn(II) to Mn(III) on δ-MnO_2 surfaces. The reactive sites could be

occupied or blocked by the reformed Mn(III) phases, resulting in much lower peak intensity at 461 cm^{-1}.

Tables:

Table S1. XPS Mn 3s multiplet splitting results for reference Mn oxides and δ-MnO_2 samples before and after reaction.

Sample	Curve 1: Mn ^{5}S (eV)	Curve 2: Mn ^{7}S (eV)	Multiplet Splitting (eV)	Mn AOS
Reference				
MnO; Mn(II)	88.44	82.75	5.69	2.00
Mn_2O_3; Mn(III)	88.54	83.15	5.39	3.00
MnO_2; Mn(IV)	88.12	83.63	4.49	4.00
Sample				
δ-MnO_2	88.30	83.55	4.75	3.58[a]
5.5-O	88.35	83.39	4.96	3.35[a]
5.5-A	88.35	83.35	5.00	3.30[a]
7.0-O	88.35	83.43	4.92	3.39[a]
7.0-A	88.30	83.38	4.93	3.38[a]
8.5-O	88.34	83.46	4.88	3.44[a]
8.5-A	88.31	83.45	4.86	3.46[a]

a – Obtained from Mn 3s multiplet splitting results: AOS = 8.95 – 1.13ΔEs, where ΔEs is the energy difference between the main peak and its satellite in Mn 3s [7].

Table S2. XPS Mn 2p3/2 fitting results of control and reacted samples.

Sample	%Mn(IV)	%Mn(III)	%Mn(II)	AOS
δ-MnO_2	67.8 ± 1.3	28.7 ± 0.1	3.5 ± 1.2	3.64 ± 0.08
5.5-O	41.4 ± 2.2	51.3 ± 2.1	7.3 ± 0.1	3.34 ± 0.15
5.5-A	42.5 ± 0.1	49.6 ± 1.2	7.9 ± 1.3	3.35 ± 0.07
7.0-O	49.2 ± 2.7	44.5 ± 3.5	6.4 ± 0.8	3.43 ± 0.23
7.0-A	49.4 ± 0.5	44.6 ± 0.2	6.0 ± 0.7	3.43 ± 0.04
8.5-O	55.3 ± 1.9	41.4 ± 3.4	3.3 ± 1.5	3.52 ± 0.21
8.5-A	53.1 ± 3.5	44.2 ± 3.1	2.7 ± 0.4	3.50 ± 0.24

Figures:

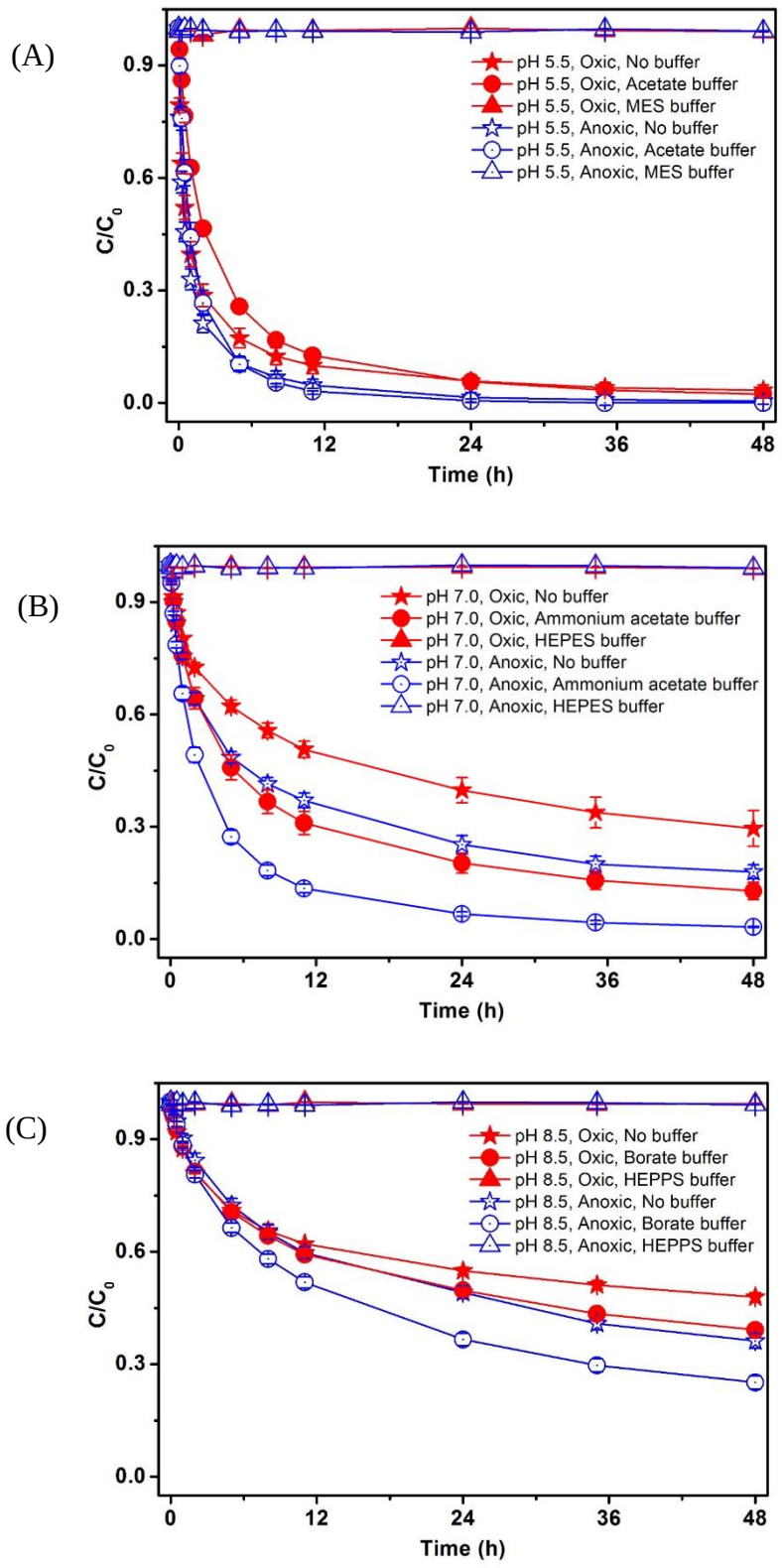

Figure S1. Phenol degradation with δ-MnO_2 at pH 5.5 (**A**), pH 7.0 (**B**), and pH 8.5 (**C**) in the presence of 10 mM acetate, ammonium acetate, borate, MES, HEPES, and HEPPS buffers, as compared to non-buffered suspensions.

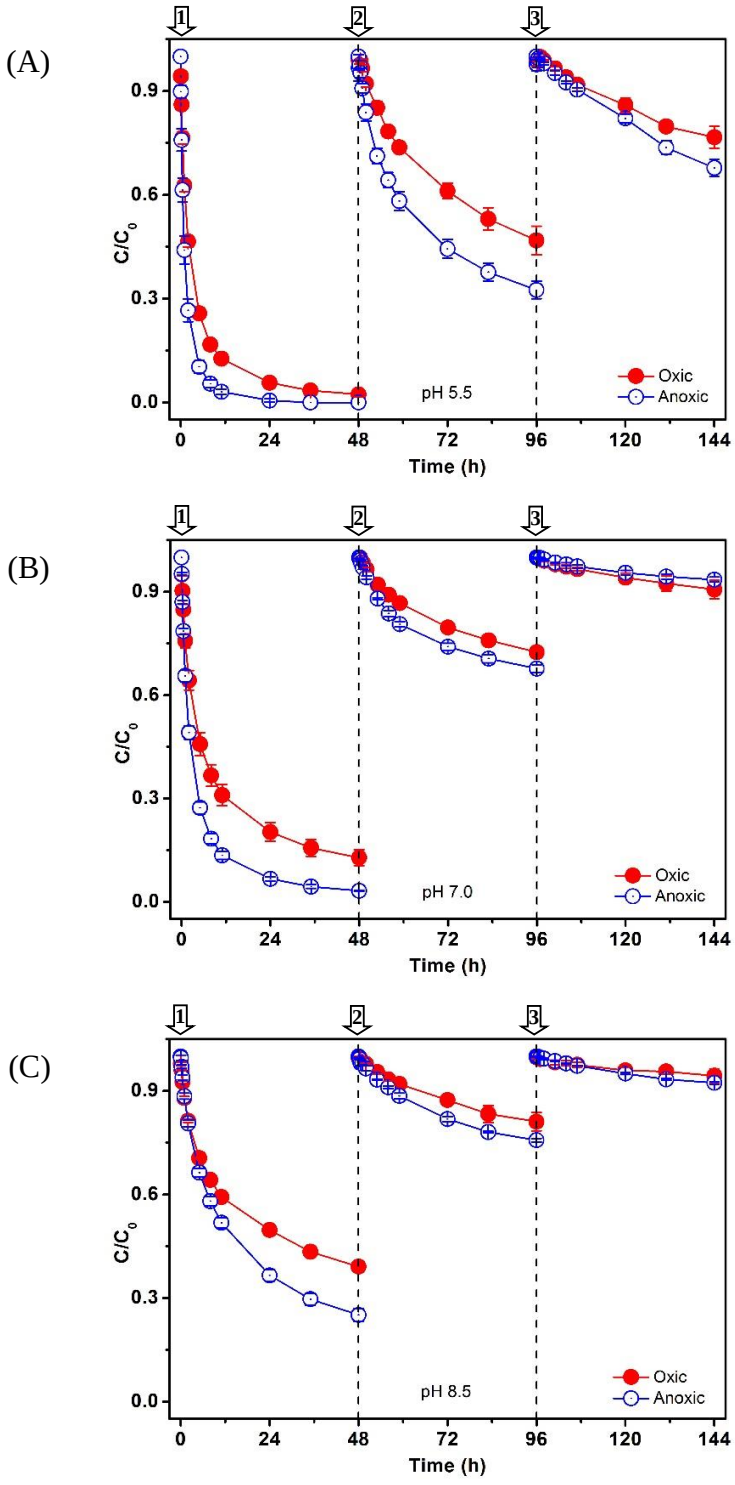

Figure S2. Degradation of phenol by δ-MnO_2 over three reaction cycles at pH 5.5 (**A**), pH 7.0 (**B**), and pH 8.5 (**C**) under both oxic and anoxic conditions ($[Phenol]_0$ = 53.2 μM, $[\delta\text{-}MnO_2]_0$ = 945.5 μM).

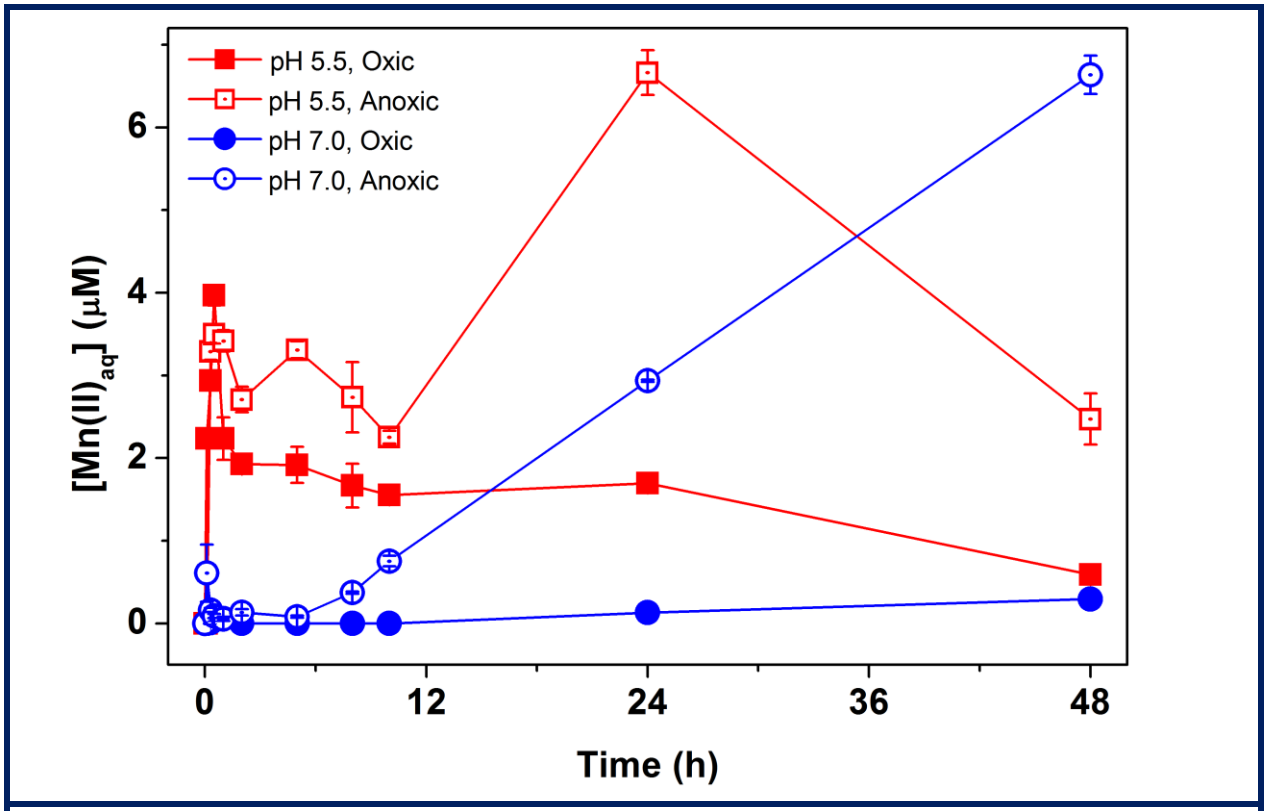

Figure S3. Concentrations of dissolved Mn during reduction of δ-MnO_2 by phenol at pH 5.5 and 7.0 under both oxic and anoxic conditions ($[Phenol]_0$ = 53.2 μM, $[\delta\text{-}MnO_2]_0$ = 945.5 μM). Note that dissolved Mn was below the detection limit (0.02 μM) at pH 8.5.

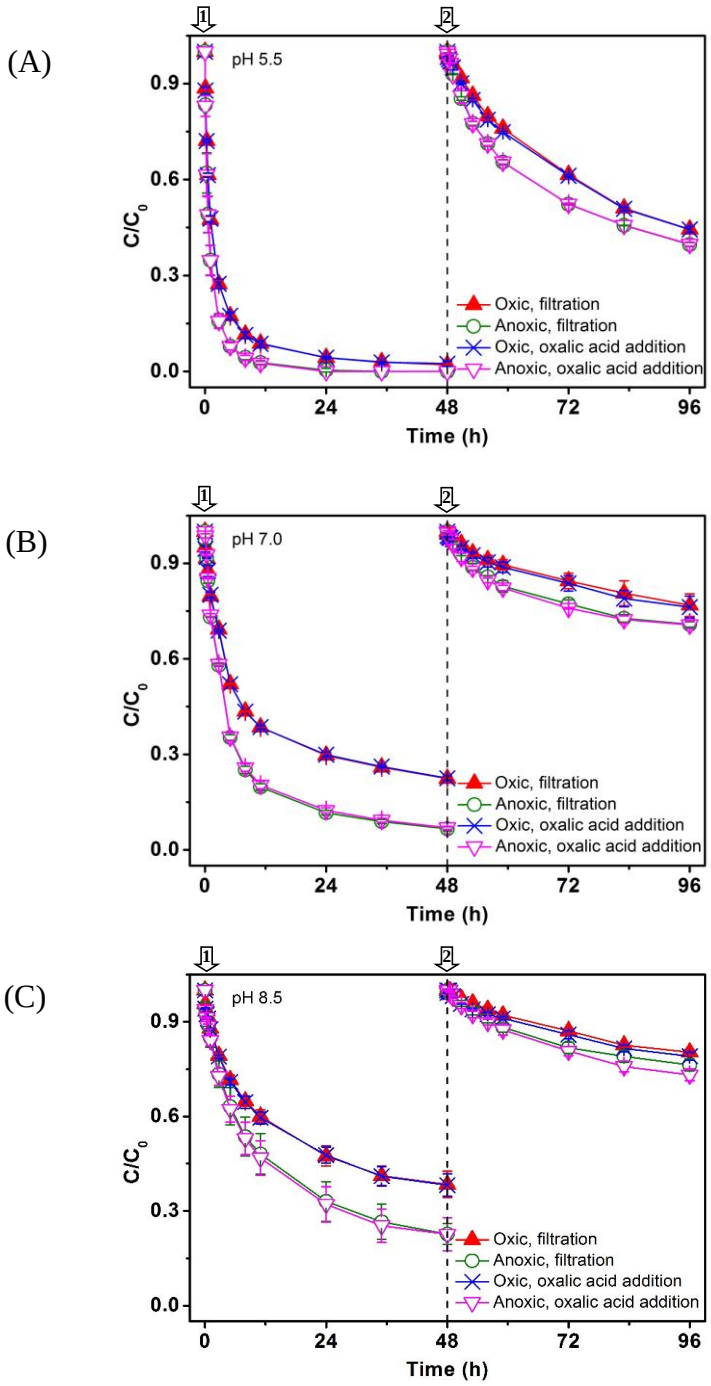

Figure S4. Sorption of phenol to δ-MnO_2 during the degradation processes at pH 5.5 (**A**), pH 7.0 (**B**), and pH 8.5 (**C**) over two reaction cycles. The concentration in samples quenched by oxalate addition corresponds to the total amount of phenol; the concentration in samples quenched by filtration represents the dissolved amount; phenol sorbed on δ-MnO_2 surface determined by the difference between the total amount and the dissolved amount.

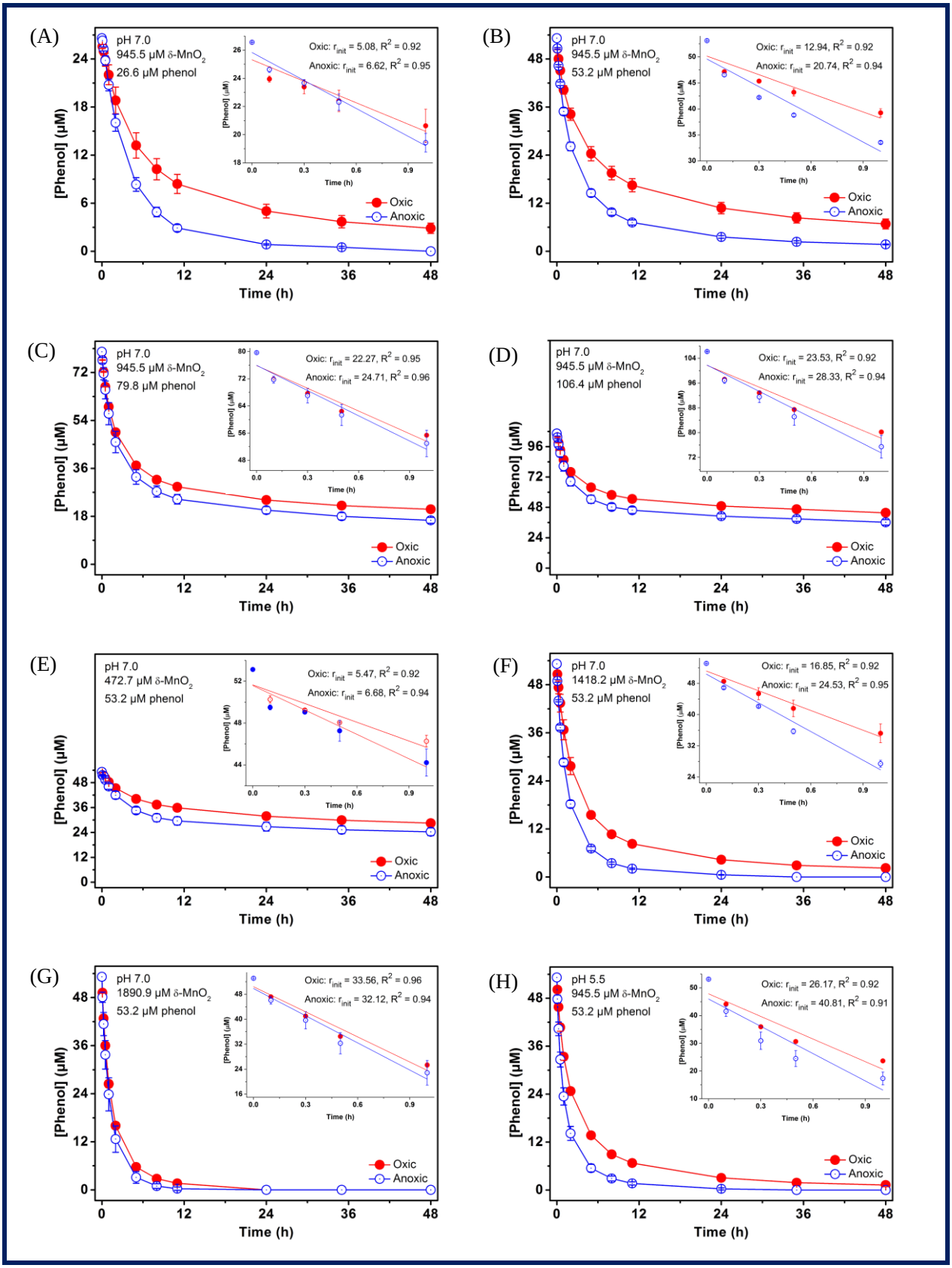
(A)
pH 7.0
945.5 μM δ-MnO2
26.6 μM phenol
Oxic: rinit = 5.08, R2 = 0.92
Anoxic: rinit = 6.62, R2 = 0.95
(B)
pH 7.0
945.5 μM δ-MnO2
53.2 μM phenol
Oxic: rinit = 12.94, R2 = 0.92
Anoxic: rinit = 20.74, R2 = 0.94
(C)
pH 7.0
945.5 μM δ-MnO2
79.8 μM phenol
Oxic: rinit = 22.27, R2 = 0.95
Anoxic: rinit = 24.71, R2 = 0.96
(D)
pH 7.0
945.5 μM δ-MnO2
106.4 μM phenol
Oxic: rinit = 23.53, R2 = 0.92
Anoxic: rinit = 28.33, R2 = 0.94
(E)
pH 7.0
472.7 μM δ-MnO2
53.2 μM phenol
Oxic: rinit = 5.47, R2 = 0.92
Anoxic: rinit = 6.68, R2 = 0.94
(F)
pH 7.0
1418.2 μM δ-MnO2
53.2 μM phenol
Oxic: rinit = 16.85, R2 = 0.92
Anoxic: rinit = 24.53, R2 = 0.95
(G)
pH 7.0
1890.9 μM δ-MnO2
53.2 μM phenol
Oxic: rinit = 33.56, R2 = 0.96
Anoxic: rinit = 32.12, R2 = 0.94
(H)
pH 5.5
945.5 μM δ-MnO2
53.2 μM phenol
Oxic: rinit = 26.17, R2 = 0.92
Anoxic: rinit = 40.81, R2 = 0.91
[Phenol] (μM)
Time (h)
Oxic
Anoxic

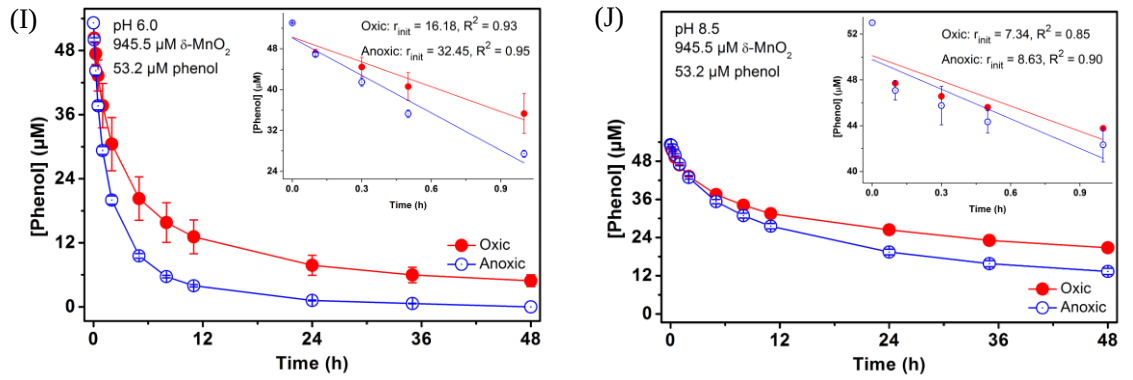

Figure S5. Effect of initial concentration of phenol (**A**, **B**, **C**, **D**), δ-MnO_2 dosage (**B**, **E**, **F**, **G**), and pH (**B**, **H**, **I**, **J**) on phenol degradation (inset is the fittings of the initial reaction rates).

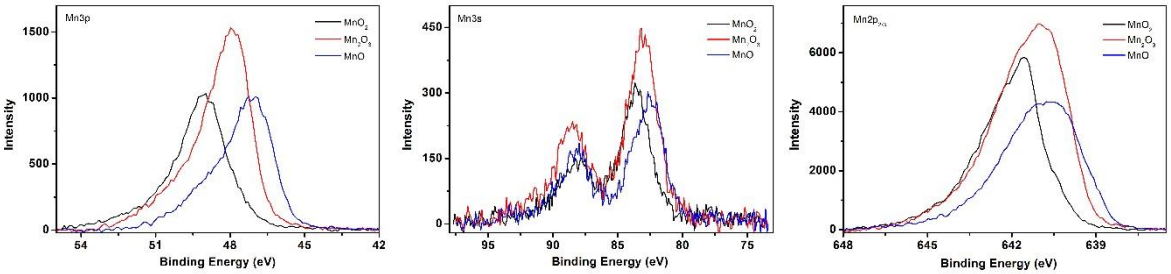

Figure S6. Mn 3p, Mn 3s, Mn 2p3/2 photo-peak for Mn(II), Mn(III), and Mn(IV) oxide standards.

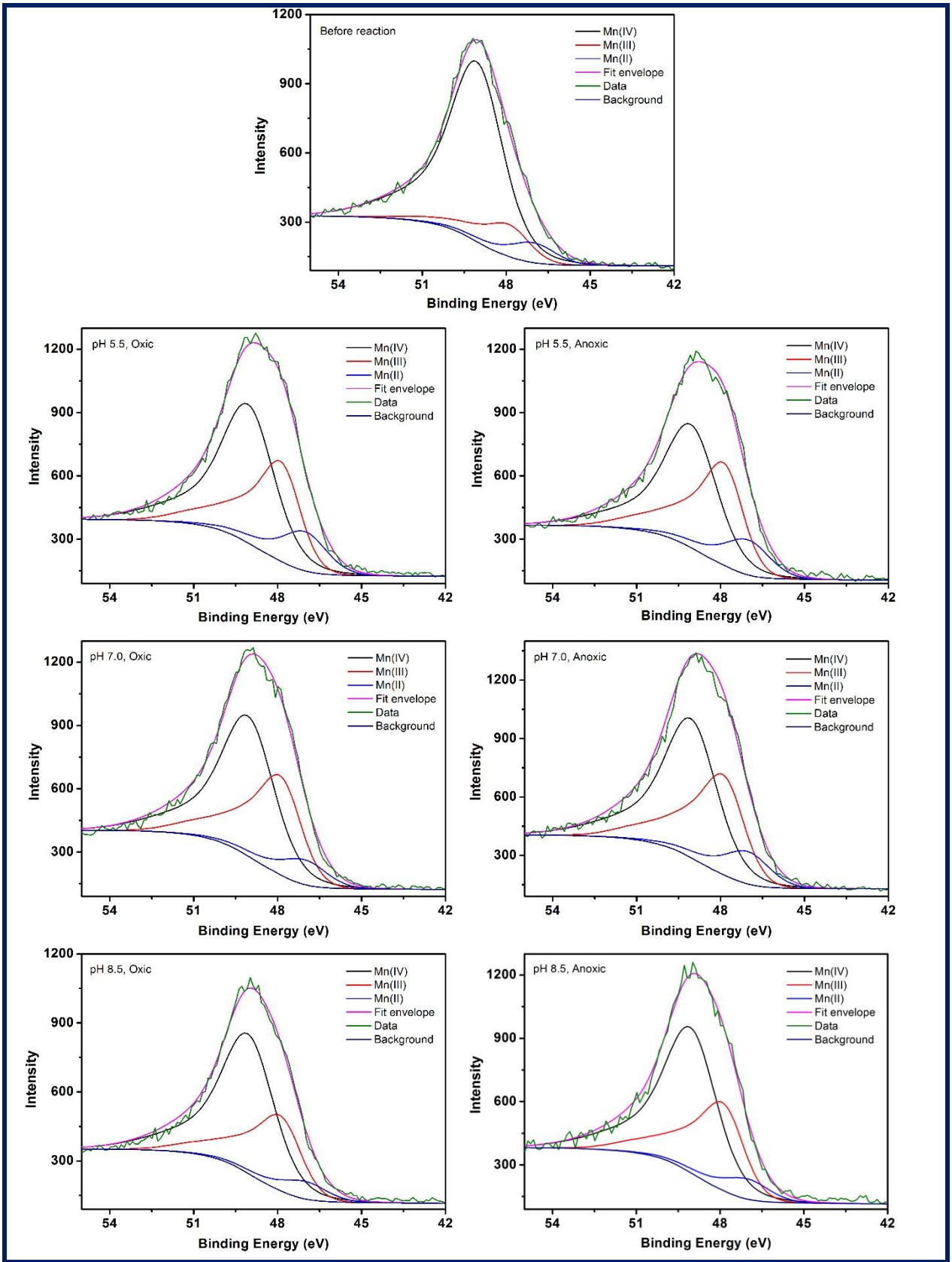

Figure S7. Fitting of Mn 3p XPS spectrum of δ-MnO_2 before and after reaction with phenol.

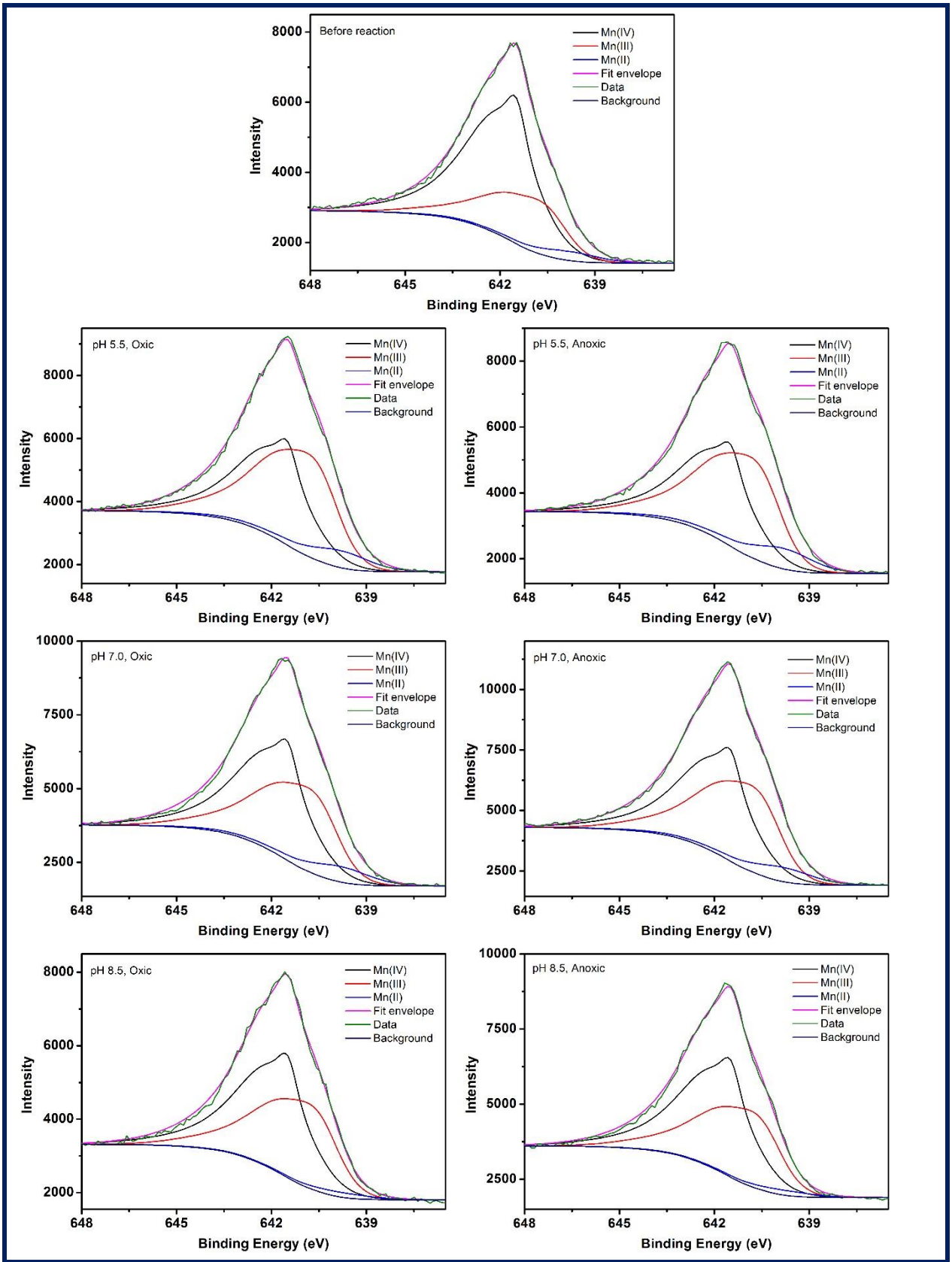

Figure S8. Fitting of Mn 2p3/2 XPS spectrum of δ-MnO_2 before and after reaction with phenol.

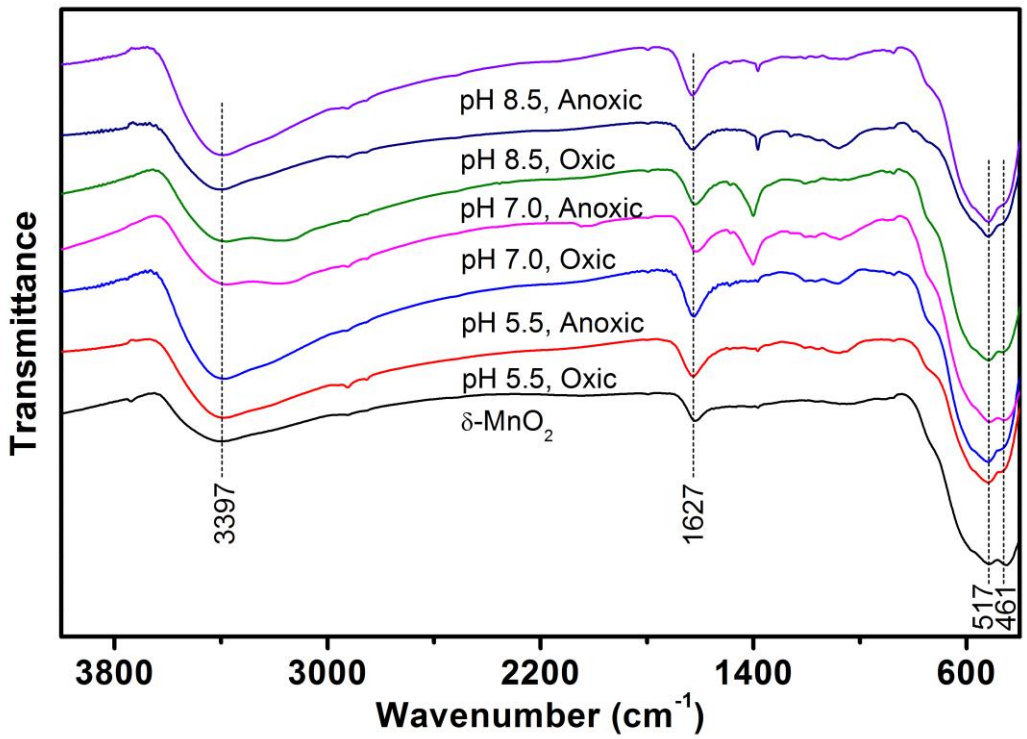

Figure S9. FTIR spectra of synthesized δ-MnO_2 before and after reduction by phenol for one cycle.

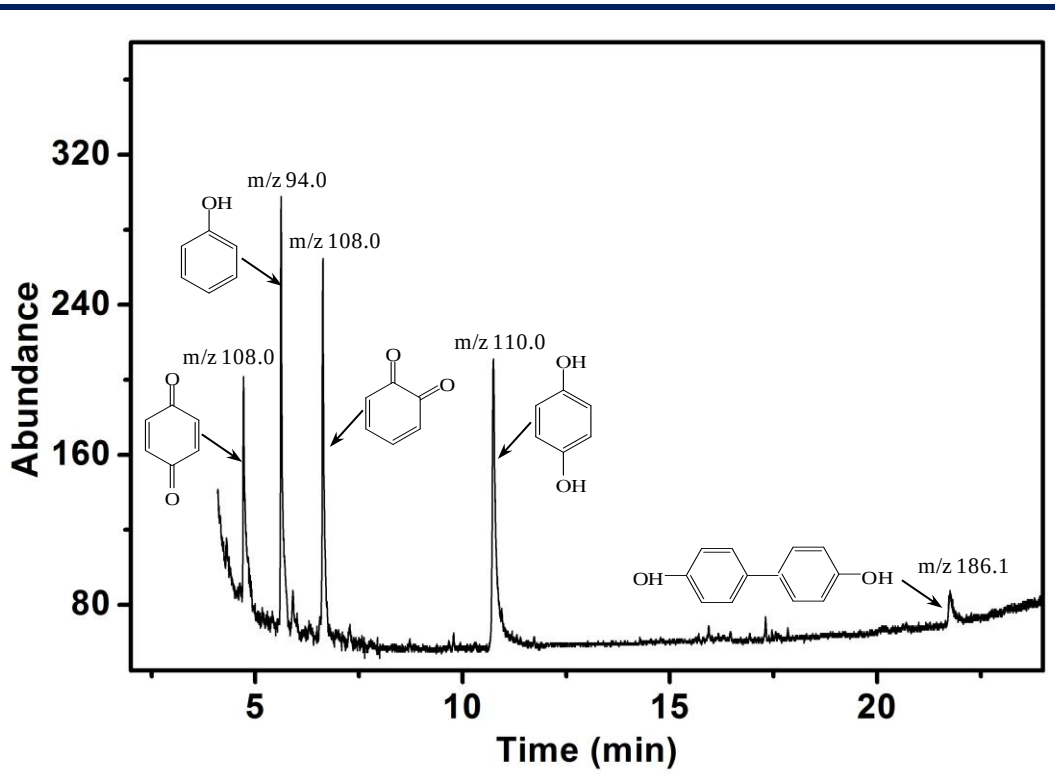

Figure S10. Degradation products of phenol after reaction with δ-MnO_2 for 35 h at pH 5.5 under anoxic conditions.

References:

1 S. Balgooyen, G. Campagnola, C. K. Remucal, M. Ginder-Vogel, Impact of bisphenol A influent concentration and reaction time on MnO2 transformation in a stirred flow reactor, *Environ. Sci.: Processes Impact*, 2019, **21**, 19-27.

2 J. Klausen, S. B. Haderlein, R. P. Schwarzenbach, Oxidation of substituted anilines by aqueous MnO_2: Effect of co-solutes on initial and quasi-steady-state kinetics, *Environ. Sci. Technol.*, 1997, **31**, 2642-2649.

3 M. Villalobos, B. Toner, J. Bargar, G. Sposito, Characterization of the manganese oxide produced by pseudomonas putida strain MnB1, *Geochim. Cosmochim. Acta*, 2003, **67**, 2649−2662.

4 N. Wang, S. Lo, Preparation, characterization and adsorption performance of cetyltrimethylammonium modified birnessite, *Appl. Surf. Sci.*, 2014, **299**, 123−130.

5 M. Händel, T. Rennert, K. U. Totsche, Synthesis of cryptomelane- and birnessite-type manganese oxides at ambient pressure and temperature, *J. Colloid Interface Sci.*, 2013, **405**, 44−50.

6 G. Chen, L. Zhao, Y. H. Dong, Oxidative degradation kinetics and products of chlortetracycline by manganese dioxide, *J. Hazard. Mater.*, 2011, **193**, 128−138.

7 J. Huang, S. Zhong, Y. Dai, C. Liu, H. Zhang, Effect of MnO_2 phase structure on the oxidative reactivity toward bisphenol A degradation, *Environ. Sci. Technol.*, 2018, **52**, 11309−11318.